

Effect of energy pooling collisions in formation of a cesium plasma by continuous wave resonance excitation

M.A. MAHMOUD^{1*}, Y.E.E. GAMAL^{2,3}

¹Physics Department, Faculty of Science, Sohag University, Sohag 82524, Egypt

²Department of Physics, Girls' Faculty of Science, King Abdul-Aziz University, Jeddah, KSA

³National Institute of Laser Enhanced Science, Cairo University, El Giza, Egypt – permanent address

*Corresponding author: hameid56@hotmail.com

The generation of plasma in cesium vapor excited by cw laser is investigated theoretically. We have developed a computational model which quantitatively explains the laser power dependences of electron energy distribution function (EEDF) and the level population densities which were created during the interaction. The energy spectra of the electrons emerging from the interaction show that the mechanisms by which electrons gain energy through the resonant system can significantly increase the density of the resonant plasma. The nonlinear behaviour of the ion current suggests that the plasma formation is initiated via collisional ionization and collisional excitation, such as associative ionization, Penning ionization, or photoionization as well as energy pooling collisions. The Cs–Cs atom collisions play important role in the formation of a highly Cs plasma with the use of a relatively low power laser to excite a resonance transition. A comparison between the behaviour of the calculated ion current as a function of a laser power is proved to be a reasonable agreement with that measured by PAPPAS *et al.* (*Appl. Spectrosc.* **54**, 2000, p. 1245). The results may be useful in designing and developing cw metal vapor lasers.

Keywords: laser, collisional ionization, energy pooling, plasma, cesium.

1. Introduction

There is a long history of studies concerning laser excitation and ionization of alkali-metal vapors [1, 2]. The absorption of laser photons in alkali-metal vapors is possible by tuning the laser frequency to the resonant transition, quasiresonant transitions, and two-photon resonant transitions. That interesting effect was further investigated by TAM and HAPPER [3, 4] in Cs vapor with extension of the technique to the cw laser quasiresonant excitation $6P \rightarrow 8D$ at 601 nm. The laser-induced fluorescence from a dense Cs vapor showed recombination continuum and plasma-broadband atomic lines [3].

In 1976 ALLEGRIANI *et al.* [5] reported that, when atomic vapors are resonantly excited by laser radiation, it is often possible to observe fluorescence from levels

lying near twice the excitation energy [5]. Such fluorescence can result from “energy-pooling” (EP) collisions in which two excited atoms collide and “pool” their energy so that one atom ends in the ground state and the other in a more highly excited state. Since energy deficits or surpluses must be taken up by kinetic energy of colliding atoms, it is clear that the strongest EP collision processes will be those where the final energy state lies near twice the excitation energy. Energy pooling collisions have been studied extensively in alkali homonuclear [6–9] and heteronuclear systems [10, 11], as well as in other metal vapors over the last 20 years. Measurements of EP cross sections at thermal energies provide important test of theoretical molecular potential curves at large internuclear distances. However, energy pooling collisions in cesium are of current interest because such collisions could be an important loss mechanism in ultracold laser traps [12, 13], in which the atomic density is very high (10^{11} to 10^{13} cm^{-3}). Recently, many experimental investigations on energy pooling processes in cesium vapors have been published [14–18]. The main purpose of these investigations is to present quantitative results for the rate coefficients and cross sections for the cesium energy-pooling process. The theoretical evaluation of laser ionization by resonant light was made by Measures and co-workers [19, 20]. In their model, called LIBORS (light ionization based on resonance saturation), the laser rapidly saturates the resonant level. Once the large pool of atoms in resonant state is created, seed electrons are generated by multiphoton ionization from the resonant level, by associative ionization, by laser-induced Penning ionization, and by other ionization processes. Free electrons rapidly gain energy through superelectric collisions with excited atoms, so that electron impact ionization from the resonant level and collisionally populated upper levels contribute to the rate of ionization together with the single-photon ionization from those upper levels. Almost complete ionization of the excited atoms occurs when a critical electron density is achieved.

Due to the importance of the energy pooling collisions in the laser interaction with cesium atom, we developed a numerical model [21, 22] by adding this process to the ionization scheme to study the kinetics of the resonant laser plasma produced when cesium vapor is excited by cw laser under the experimental conditions of PAPPAS *et al.* [23]. The formulation of the model, is described in the following section, which incorporates associative ionization, Penning ionization, electron impact excitation and ionization, photoionization, excited atom-excited atom collisions, and radiative recombination, as well as three body recombinations. The energy-level diagram of cesium atom involved in the model is shown in Fig. 1.

2. Theoretical formulation of the model

2.1. The rate equations

A set of differential equations for instantaneous population densities of different states, electron density as a function of electron energy, together with the normalization

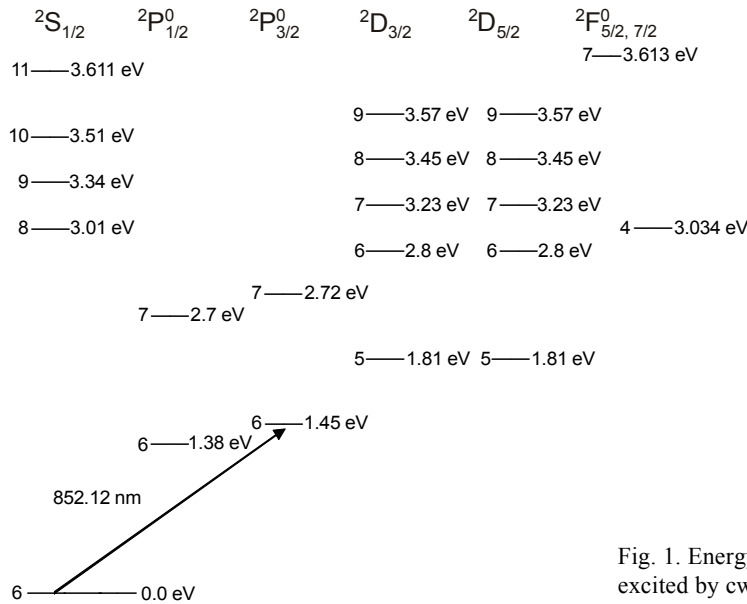


Fig. 1. Energy level diagram of Cs atom excited by cw laser.

conditions, are developed and solved iteratively. We will first describe the basic equations.

The rate of change of instantaneous population density $N(6s)$ of a particular state $6s$ is given by:

$$\begin{aligned} \frac{dN(6s)}{dt} = & N(6p)(R_{21} + A_{21}) - N(6s)R_{12} + \int n_e(\varepsilon)N(6p)K_{21}(\varepsilon)d\varepsilon + \\ & - \int n_e(\varepsilon)N(6s)K_{12}(\varepsilon)d\varepsilon + N(6p)N(n)K_{\text{PI}} + N^2(6p)\frac{K_{\text{EP1}}}{2} + \\ & + N^2(5d)\frac{K_{\text{EP2}}}{2} - \int N(6s)n_e(\varepsilon)K(\varepsilon)_{1c}d\varepsilon \dots \end{aligned} \quad (1)$$

The rate of change of the resonance state $6p$ population is given by:

$$\begin{aligned} \frac{dN(6p)}{dt} = & N(6s)R_{12} - N(6p)(R_{21} + A_{21}) - \int n_e(\varepsilon)N(6p)K_{21}(\varepsilon)d\varepsilon + \\ & + \int n_e(\varepsilon)N(6s)K_{12}(\varepsilon)d\varepsilon - N^2(6p)\frac{K_{\text{AI}}}{2} - N(6p)N(n)K_{\text{PI}} + \\ & - N^2(6p)\frac{K_{\text{EP1}}}{2} - N(6p)\sigma_{2c}^{(2)}F^2 - \int N(6p)n_e(\varepsilon)K_{2c}(\varepsilon)d\varepsilon \dots \end{aligned} \quad (2)$$

The rate of change of the population density of the high-lying nl states is given by:

$$\begin{aligned} \frac{dN(n)}{dt} = & \sum_{n>m} n_e(\varepsilon) N(n) K_{nm}(\varepsilon) - \sum_{m>n} n_e(\varepsilon) N(n) K_{mn}(\varepsilon) - \sum_{n>m} N(n) A_{nm} + \\ & - \sum_n n_e(\varepsilon) N(n) K_{nc}(\varepsilon) - \sum_n N(6p) N(n) K_{PI} + N^2(6p) \frac{K_{EP1}}{2} + \\ & + N^2(5d) \frac{K_{EP2}}{2} - \sum_{n>2} N(n) \sigma_{nc}^{(1)} F + \\ & + N(Cs^+) n_e(\varepsilon) \sum_n [n_e(\varepsilon) K_{cn}(\varepsilon) + K_{RD}(\varepsilon)] \dots \end{aligned} \quad (3)$$

Where A_{21} represents the Einstein coefficient for spontaneous emission, R_{21} represents the stimulated emission-rate coefficients for the resonance transition and is given by

$$R_{21} = \frac{\sigma_{21} I(\nu)}{E_{21}} \dots \quad (4)$$

(while σ_{21} is the cross section for the pumping of the $6s-6p$ transition whose energy is E_{21} and $I(\nu)$ is the laser irradiance); K_{nm} is the rate coefficient for an electron collision-induced transition from level n to m , K_{1c} represents the rate coefficient of electron impact ionization for the $6s$, K_{2c} represents the rate coefficient of electron impact ionization for the $6p$, K_{nc} represents the rate coefficient of electron impact ionization for the nl state, K_{AI} represents the rate coefficient for associative ionization process, K_{PI} represents the rate coefficient for Penning ionization process, K_{EP1} represents the rate coefficient for energy pooling of $6p-6p$ collisions, K_{EP2} represents the rate coefficient for energy pooling of $5d-5d$ collisions, $\sigma_{nc}^{(1)}$ represents the single-photon ionization cross section for level n , $\sigma_{2c}^{(2)}$ represents the two-photon resonance state cross section, K_{cn} represents the rate coefficient for three body recombination into state n , K_{RD} represents the rate coefficient for radiative recombination into state n , F represents laser photon flux density, $N(n)$ represents the population density of highly excited states, $N(Cs^+)$ represents the atomic ion density, $n_e(\varepsilon)$ represents the electron density as a function of electron energy ε .

The time dependence of the Boltzmann equation, which gives the actual energy distribution function for the free electrons created due to these processes, is given by

$$\begin{aligned} \frac{dn_e(\varepsilon)}{dt} = & \sum_{m>n} n_e(\varepsilon) N(n) K_{mn}(\varepsilon) - \sum_{n>m} n_e(\varepsilon) N(n) K_{nm}(\varepsilon) + \sum_n n_e(\varepsilon) N(n) K_{nc}(\varepsilon) + \\ & + \sum_n N(6p) N(n) K_{PI} + N^2(6p) \frac{K_{AI}}{2} + N(6p) \sigma_{2c}^{(2)} F^2 + \\ & + \sum_{n>2} N(n) \sigma_{nc}^{(1)} F - N(Cs^+) n_e(\varepsilon) \sum_n [n_e(\varepsilon) K_{cn}(\varepsilon) + K_{RD}(\varepsilon)] \dots \end{aligned} \quad (5)$$

The normalization conditions are:

$$\begin{aligned} N_0 &= \sum_n N(n) + N(\text{Cs}^+) \dots \\ \int_0^\infty n_e(\varepsilon) &= 1 \quad (6) \\ \int_0^\infty n_e(\varepsilon) d\varepsilon &= N_e \end{aligned}$$

where N_e is the number density of electrons and N_0 is the vapor density of Cs.

While the time evolution of the atomic and molecular ions is given by

$$\begin{aligned} \frac{dN(\text{Cs}^+)}{dt} &= \sum_n N(6p)N(n)K_{\text{PI}} + \sum_n n_e(\varepsilon)N(n)K_{nc}(\varepsilon) + N(6p)\sigma_{2c}^{(2)}F^2 + \\ &+ \sum_{n>2} N(n)\sigma_{nc}^{(1)}F - N(\text{Cs}^+)n_e(\varepsilon)\sum_n \left[n_e(\varepsilon)K_{cn}(\varepsilon) + K_{\text{RD}}(\varepsilon) \right] \dots \quad (7) \end{aligned}$$

$$\frac{dN(\text{Cs}_2^+)}{dt} = N^2(6p)\frac{K_{\text{AI}}}{2} \quad (8)$$

The factor 1/2 in associative ionization and energy pooling processes in the above mentioned equations corrects for possible double counting of each colliding pair of identical particles [24].

2.2. Cesium data

The main problem in developing a realistic computer model is the lack of reliable experimental data on the rate coefficients for various collisional and radiative processes. In the case of cesium, the problem is particularly severe. However, we have used analytical formulas for electron collisional excitation and deexcitation discrete states, as well as for the electron collisional ionization (see [21]). An estimate of the Penning ionization rate coefficient for cesium atom cannot be found in the literature. Thus, we have used K_{PI} from Ref. [26]. On the other hand, the values of the rate coefficients for the associative ionization, Penning ionization and energy pooling collisions are in Tab. 1. The photoionizatin cross sections $\sigma(nl, \lambda)$ are indicated in Tab. 2.

3. Results and discussion

A set of Eqs. (1)–(8), which was mentioned previously, is solved numerically by a fourth-order Runge–Kutta technique under the experimental conditions of PAPPAS *et al.* [23]. In their experiment, they examined a plasma formed by a relatively

T a b l e 1. Associative ionization, Penning ionization and energy pooling collisions rate coefficients of cesium atom.

Process	Rate coefficients [cm ³ sec ⁻¹]	Reference
1) Associative ionization		
Cs(6p) + Cs(6p) → Cs ₂ ⁺ (Σ _{g,v}) + e	(2±0.2)×10 ⁻¹³	[25]
2) Penning ionization		
Cs(6p) + Cs(nl) → Cs ⁺ + Cs(6s) + e	≈ 1×10 ⁻¹⁰	[26]
3) Energy pooling collisions		
Cs(6p _{3/2}) + Cs(6p _{3/2}) → Cs(7p _{1/2}) + Cs(6s _{1/2})	5.59×10 ⁻¹²	[14]
Cs(6p _{3/2}) + Cs(6p _{3/2}) → Cs(7p _{3/2}) + Cs(6s _{1/2})	1.81×10 ⁻¹²	[14]
Cs(6p _{3/2}) + Cs(6p _{3/2}) → Cs(6d _{3/2}) + Cs(6s _{1/2})	1.43×10 ⁻¹⁰	[14]
Cs(6p _{3/2}) + Cs(6p _{3/2}) → Cs(6d _{5/2}) + Cs(6s _{1/2})	1.89×10 ⁻¹⁰	[14]
Cs(6p _{3/2}) + Cs(6p _{3/2}) → Cs(4f _{5/2}) + Cs(6s _{1/2})	1.23×10 ⁻¹¹	[14]
Cs(6p _{3/2}) + Cs(6p _{3/2}) → Cs(4f _{7/2}) + Cs(6s _{1/2})	2.04×10 ⁻¹¹	[14]
Cs(6p _{3/2}) + Cs(6p _{3/2}) → Cs(8s _{1/2}) + Cs(6s _{1/2})	1.74×10 ⁻¹¹	[14]
Cs(6p _{1/2}) + Cs(6p _{1/2}) → Cs(7p _{1/2}) + Cs(6s _{1/2})	2.14×10 ⁻¹¹	[14]
Cs(6p _{1/2}) + Cs(6p _{1/2}) → Cs(7p _{3/2}) + Cs(6s _{1/2})	5.35×10 ⁻¹¹	[14]
Cs(6p _{1/2}) + Cs(6p _{1/2}) → Cs(6d _{3/2}) + Cs(6s _{1/2})	5.54×10 ⁻¹⁰	[14]
Cs(6p _{1/2}) + Cs(6p _{1/2}) → Cs(6d _{5/2}) + Cs(6s _{1/2})	2.7×10 ⁻¹⁰	[14]
Cs(6p _{1/2}) + Cs(6p _{1/2}) → Cs(4f _{5/2}) + Cs(6s _{1/2})	≈ 2.8×10 ⁻¹¹	[14]
Cs(6p _{1/2}) + Cs(6p _{1/2}) → Cs(4f _{7/2}) + Cs(6s _{1/2})	≈ 2.7×10 ⁻¹¹	[14]
Cs(6p _{1/2}) + Cs(6p _{1/2}) → Cs(8s _{1/2}) + Cs(6s _{1/2})	1.39×10 ⁻¹²	[14]
Cs(5d) + Cs(5d) → Cs(9d) + Cs(6s)	4.1×10 ⁻¹²	[18]
Cs(5d) + Cs(5d) → Cs(11s) + Cs(6s)	1.6×10 ⁻¹⁰	[18]
Cs(5d) + Cs(5d) → Cs(7f) + Cs(6s)	3.6×10 ⁻¹⁰	[18]

T a b l e 2. Photoionization cross sections of excited levels of cesium atom.

Level	Wavelength [nm]	Cross section [Mb]	Reference
6p	496.5	18.6±1.5	[27]
7s	540.0	1.14±1	[28]
7p	455.5	8.8 ±1.6	[29]

low irradiation continuous-wave (cw) laser. The Ti:sapphire laser was operated with a power output of 75–150 mW and linewidth of 2 GHz (0.005 nm at 852.12 nm) is tuned to the 852.11 nm ($6s_{1/2} \rightarrow 6p_{3/2}$) resonance transition of Cs. In addition to the atomic number density of cesium $\approx 10^{12} \text{ cm}^{-3}$ at temperature 350 K.

3.1. The time evolution of the electron energy distribution function

In Figure 2 the calculated electron energy distribution function (EEDF) at a laser power of 150 mW is shown at various time intervals, namely 1, 5, 10, 50 and 100 ns, respectively. From this figure we notice that the spectral structure is observed with

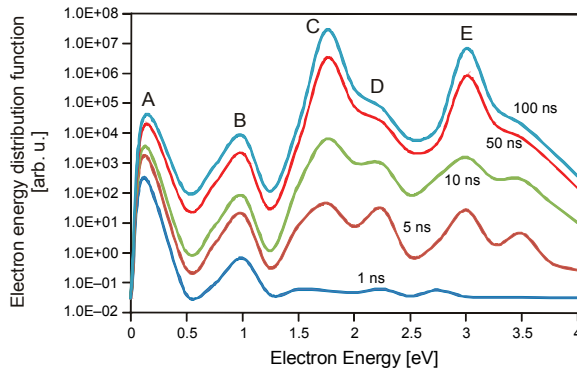


Fig. 2. Time development of the electron energy distribution function in cesium vapor excited with cw laser at a laser power of 150 mW.

certain peaks (A, B, C, D and E) lying at energies 0.12, 1, 1.75, 2.25 and 3 eV, respectively. Inspecting these curves, we attributed the peak labeled A to associative ionization (AI) process, since in this reaction the relative kinetic energy of the electron is typically much less than 0.1 eV (the difference of the binding energy of the molecular ion Cs_2^+ and the ionization energy of the $\text{Cs}(6p)$ state). The peaks B and C correspond to the electrons produced by Penning ionization process or photoionization process, in which for Penning ionization process, collisions of $\text{Cs}(nl)$ and $\text{Cs}(6p)$ atoms, with respectively, $nl = 7p, 6d, 4f, 8s, 9d, 11s$ and $7f$: $\text{Cs}(6p) + \text{Cs}(nl) \rightarrow \text{Cs}^+ + \text{Cs}(6s) + e(E_{6p} - E_b(nl))$, where $E_b(nl)$ is the binding energy of the electron in the nl state. The nl states are populated in the energy pooling collisions [14, 18], while the peaks D and E are attributed to the superelastic collisions (1SEC and 2SEC) between the free electrons produced by associative ionization and Penning ionization processes with atoms in the $\text{Cs}(6p)$ state, each of which boosts their by 1.45 eV: $\text{Cs}(6p) + e(\varepsilon) \rightarrow \rightarrow \text{Cs}(6s) + e(\varepsilon + 1.45 \text{ eV})$.

The effect of energy pooling collisions on the electron energy distribution function is indicated in Fig. 3. From this figure we note that the value of EEDF with energy pooling collision process is higher than the value of EEDF without energy pooling

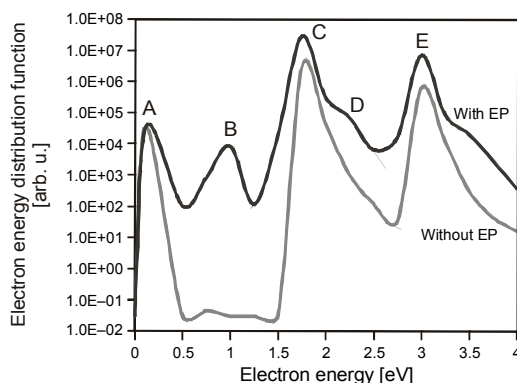


Fig. 3. Comparison between EEDF with EP and without EP.

collision. This behavior confirms the important role of the energy pooling collisions in the populated, highly excited states nl for the Penning ionization process. Moreover, the EEDF at different time intervals (Figs. 2 and 3) confirms the experimental observations of DE TOMASI *et al.* [15] and PAPPAS *et al.* [23] who reported that the nl states might be populated by recombination or excitation transfer collisions involving electrons produced by associative, Penning ionization, or photoionization processes.

3.2. The time evolution of the molecular ion Cs_2^+ and the atomic ion Cs^+

The growth rate of Cs_2^+ and Cs^+ as a function of time is illustrated in Fig. 4 at laser power equal to 150 mW. From this figure we can see that the density of Cs_2^+ and Cs^+ shows a fast increase during the period 1 ns up to 20 ns followed by a linear increase up to 30 ns. Immediately after this time the density of the molecular ion and atomic ion shows a slow increase during the late stages of the interaction. The explanation of

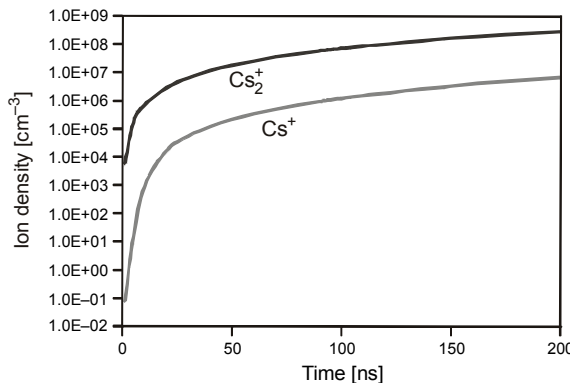


Fig. 4. The time evolution of molecular ion Cs_2^+ and the atomic ion Cs^+ at a laser power equal to 150 mW.

the linear growth can be described as follows. During the early stages, the Cs_2^+ and Cs^+ are created at a high rate through the associative ionization and Penning ionization processes, respectively. Beyond this time, the growth rate of the molecular ion and the atomic ion becomes slower due to the competition between the generation of the electrons through Penning ionization or photoionization, as well as collisional ionization of ground and excited states and the losses of the ions by radiative recombination and three recombination processes.

3.3. The dependence of the Cs_2^+ and the Cs^+ on the laser power

The molecular ion and the atomic ion densities as a function of laser power at different times are shown in Figs. 5 and 6. From this figures we note that, as the laser power increases, the Cs_2^+ and Cs^+ densities increase and the curves show almost the same behavior with descending values of the laser power for different periods of irradiation time. Moreover, at high laser power greater than 100 mW we note a very fast increase in the ions density at irradiation time equal to 100 ns. This behavior confirms that

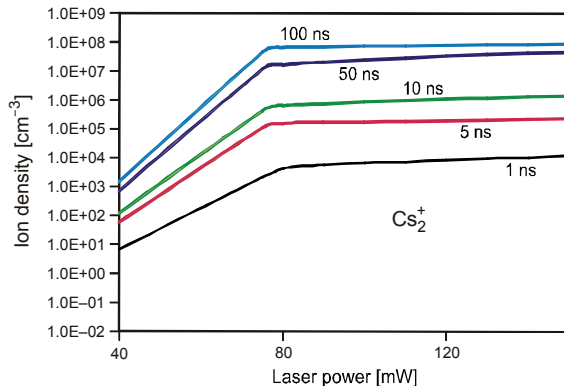


Fig. 5. The molecular ion density as a function of laser power at various times.

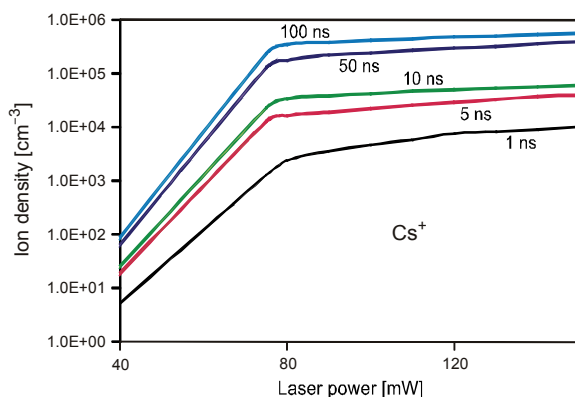


Fig. 6. The dependence of the atomic ion density on the laser power for different periods of time.

the main processes for producing the molecular ion and the atomic ion are the associative ionization and Penning ionization, respectively.

3.4. The dependence of the highly excited states on the laser power

The calculated values of the population density of four selected highly excited states ($7p$, $6d$, $8s$ and $9d$) are plotted as a function of laser power in Fig. 7. From this figure we note that, as the laser power increases, the population density of states increases and the curves show almost the same behavior with descending values of the laser power. This may be due to the continuous population of these levels via energy pooling collisions process between two up $6p$ cesium atom [15, 23, 30].

3.5. The time evolution of the highly excited states

The growth rate of the population density of the highly excited state $7p$, $6d$, $8s$ and $9d$ of cesium atom as a function of time at laser power equal to 150 mW is illustrated in Fig. 8. From this figure we can see that the growth rate of all excited states increases sharply during the early stages of the interaction formation. This behavior indicates

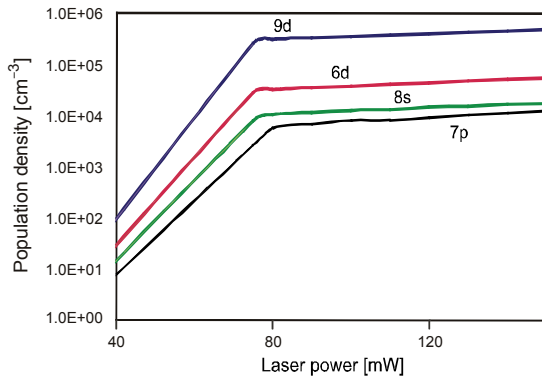


Fig. 7. The dependence of highly excited states $\text{Cs}(nl)$ which populated via energy pooling collisions on the laser power.

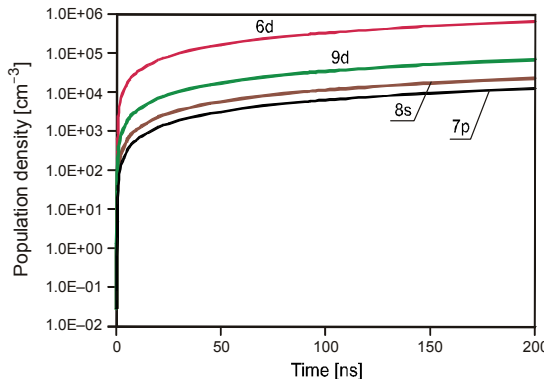


Fig. 8. The time evolution of the highly excited states $\text{Cs}(nl)$ at a laser power equal to 150 mW.

the important role of the energy pooling collisions process in populating these levels. These four levels have been chosen deliberately because there are measured values for their energy pooling collisions rate coefficients (Tab. 1). Moreover, the growth rate of $6d$ state exceeds that for the $7p$, $8s$ and $9d$ states, as indicated in Fig. 8. This confirms the rate coefficients value of the energy pooling collisions for these states observed experimentally [14, 18]. To confirm these results, we compared our calculations of the ion current with the ion current obtained experimentally by PAPPAS *et al.* [23].

3.6. Comparison between the ion current measured by PAPPAS *et al.* [23] and the ion current calculated by the model

The ion current was calculated in order to determine the degree of ionization in the plasma. Also, the ion current generated in the plasma was calculated as a function of laser intensity in order to ascertain whether or not the plasma was generated by multiphoton process.

According to CHERET *et al.* [31] and MAHMOUD [32], the basic formula of the ion current of the atomic ion is given by

$$I_{\text{PI}} = eV K_{\text{PI}} N(6s) N(n) \quad (9)$$

$$I_{\text{PHO}} = eV(P/S)(\lambda/hc)\sigma(nl, \lambda) \quad (10)$$

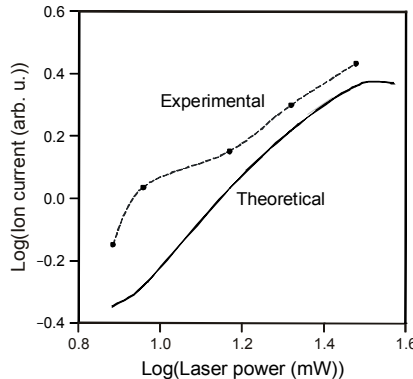


Fig. 9. Comparison between the ion current measured by PAPPAS *et al.* [23] and that calculated by our model.

while the ion current of the molecular ion is given by

$$I_{AI} = eVK_{AI}N^2(6p) \quad (11)$$

In these expressions, I_{PI} , I_{PHO} and I_{AI} represent the ion current for Penning ionization, photoionization and associative ionization processes, respectively; e , c , h are the usual notations for the elementary charge, the speed of light and the Planck constant; V is the interaction volume which is equal to the overlapping volume of the laser beams; P and S are the laser power and the beam section, respectively.

A log-scale plot of the ion current as a function of laser intensity is shown in Fig. 9. The slope of the log–log plot experimentally is 1.004, while the slope in our model is 1.241, indicating that the mechanism is due to a single photon excitation [23]. The behavior of the ion current curve showed a linear and a quadric dependence of the ion current on the laser power. The linear part comes from the photoionization and the quadratic part comes from Penning ionization processes. This can be explained by the dominant mechanisms for producing the atomic ion current, which are the Penning ionization or the photoionization processes [30]. In general, the calculated ion currents for the plasma generated in laser excited cesium vapor have approximately the same shape as those measured by PAPPAS *et al.* [23].

4. Conclusions

At this point we can conclude that the EEDF at different time intervals confirms the experimental observations of the formation of a highly ionized Cs plasma with the use of a relatively low laser power to excite a resonance transition [23]. The irradiance of the Ti:sapphire laser was on the order of 1.5 W/cm^2 , which is significantly lower than the irradiance used in conventional laser-coupled plasmas (MW/cm^2 – GW/cm^2). The major mechanism for the formation of this plasma is associative ionization and Penning ionization, especially at the early stages of the interaction. The linear dependence of the molecular density and the atomic density on the laser power indicates that a one photon process is responsible for the plasma formation.

The nonlinear dependence of the electron energy distribution function on the laser power indicates that a collisional process, such as associative ionization, Penning ionization, as well as energy pooling collisions (which play an important role in populating the highly excited states), forms the plasma. The model presents the preliminary results concerning the successful coupling of low-irradiance cw laser light to a plasma via a resonance process.

References

- [1] LUCATORTO T.B., McILRATH T.J., *Laser excitation and ionization of dense atomic vapors*, Applied Optics **19**(23), 1980, pp. 3948–3956.
- [2] LUCATORTO T.B., McILRATH T.J., *Efficient laser production of a Na^+ ground-state plasma column: Absorption spectroscopy and photoionization measurement of Na^+* , Physical Review Letters **37**(7), 1976, pp. 428–431.
- [3] TAM A.C., HAPPER W., *Plasma production in a Cs vapor by a weak CW laser beam at 6010 \AA* , Optics Communications **21**(3), 1977, pp. 403–407.
- [4] TAM A.C., *Quasiresonant laser-produced plasma: An efficient mechanism for localized breakdown*, Journal of Applied Physics **51**(9), 1980, pp. 4682–4687.
- [5] ALLEGRENI M., ALZETTA G., KOPYSTYNKA A., MOI L., ORRIOLS G., *Electronic energy transfer induced by collision between two excited sodium atoms*, Optics Communications **19**(1), 1976, pp. 96–99.
- [6] ALLEGRENI M., GABBANINI C., MOI L., *Energy pooling processes in laser excited alkali vapors: An update on experiments*, Le Journal de Physique Colloques **46**(C1), 1985, pp. 61–73.
- [7] ALLEGRENI M., GABBANINI C., MOI L., COLLE R., *Cross-section measurement and theoretical evaluation for the energy-transfer collision $\text{Na}(3P) + \text{Na}(3P) \rightarrow \text{Na}(4F) + \text{Na}(3S)$* , Physical Review A **32**(4), 1985, pp. 2068–2076.
- [8] DAVIDSON S.A., KELLY J.F., GALLAGHER A., *Final state distribution for $\text{Na}(3P_J) + \text{Na}(3P_J) \rightarrow \text{Na}(nL_{J''}) + \text{Na}(3S_{1/2})$ collisional excitation transfer*, Physical Review A **33**(6), 1986, pp. 3756–3766.
- [9] CHUN HE, BERNHEIM R.A., *Energy transfer and energy pooling from $2^2P_{3/2, 1/2}$ excited Li atoms in Li vapor*, Chemical Physics Letters **190**(5), 1992, pp. 494–496.
- [10] GOZZINI S., ABDULLAH S.A., ALLEGRENI M., CERMONCINI A., MOI L., *Heteronuclear energy pooling collisions: The $\text{Na}(3P) + \text{K}(4P)$ reaction*, Optics Communications **63**(2), 1987, pp. 97–102.
- [11] GABBANINI C., GOZZINI S., SQUADRITO G., ALLEGRENI M., MOI L., *Energy-pooling collisions for $\text{K}(4P) + \text{Rb}(5P)$ and $\text{Na}(3P) + \text{Rb}(5P)$ heteronuclear systems*, Physical Review A **39**(12), 1989, pp. 6148–6153.
- [12] FUSO F., CIAMPINI D., ARIMONDO E., GABBANINI C., *Ion processes in the photoionization of laser cooled alkali atoms*, Optics Communications **173**(1–6), 2000, pp. 223–232.
- [13] AYMER M., AZIZI S., DULIEU O., *Model-potential calculations for ground and excited Σ states of Rb_2^+ , Cs_2^+ and RbCs^+ ions*, Journal of Physics B **36**(24), 2003, pp. 4799–4812.
- [14] JABBOUR Z.J., NAMOTKA R.K., HUENNEKENS J., ALLEGRENI M.M., MILOSEVIC S., DE TOMASI F., *Energy pooling collisions in cesium: $6P_J + 6P_J \rightarrow 6S + (nl = 7P, 6D, 8S, 4F)$* , Physical Review A **54**(2), 1996, pp. 1372–1384.
- [15] DE TOMASI F., MILOSEVIC S., VERKERK P., FIORETTI A., ALLEGRENI M., JABBOUR Z.J., HUENNEKENS J., *Experimental study of caesium $6P_J + 6P_J \rightarrow 7P_J + 6S$ energy pooling collisions and modeling of the excited atom density in the presence of optical pumping and radiation trapping*, Journal of Physics B **30**(21), 1997, pp. 4991–4998.
- [16] VADLA C., *Energy pooling in cesium vapor $\text{Cs}^*(6P_J) + \text{Cs}^*(6P_J) \rightarrow \text{Cs}(6S) + \text{Cs}^{**}(6D)$* , The European Physical Journal D **1**(3), 1998, pp. 259–264.
- [17] HOON-SOO KANG, JAE-PIL KIM, CHA-HWAN OH, PILL-SOO KIM, *Energy pooling collision in Cs atomic vapor*, Journal of the Korean Physical Society **40**(2), 2002, pp. 220–223.

- [18] QIAN WANG, YIFAN SHEN, KANG DAI, *Rate coefficients measurement for the energy-pooling collisions $Cs(5D) + Cs(5D) \rightarrow Cs(6S) + Cs(nl = 9D, 11S, 7F)$* , Optics Communications **281**(8), 2008, pp. 2112–2119.
- [19] MEASURES R.M., *Efficient laser ionization of sodium vapor – A possible explanation based on superelastic collisions and reduced ionization potential*, Journal of Applied Physics **48**(7), 1977, pp. 2673–2675.
- [20] MEASURES R.M., CARDINAL P.G., *Laser ionization based on resonance saturation – a simple model description*, Physical Review A **23**(2), 1981, pp. 804–815.
- [21] MAHMOUD M.A., *Electron energy distribution function in laser-excited rubidium atoms*, Journal of Physics B **38**(10), 2005, pp. 1545–1556.
- [22] MAHMOUD M.A., GAMAL Y.E.E., ABD EL-RAHMAN H.A., *Ion formation in laser-irradiated cesium vapor*, Journal of Quantitative Spectroscopy and Radiative Transfer **102**(2), 2006, pp. 241–250.
- [23] PAPPAS D., SMITH B.W., OMENETTO N., WINEFORDNER J.D., *Formation of a cesium plasma by continuous-wave resonance excitation*, Applied Spectroscopy **54**(8), 2000, pp. 1245–1249.
- [24] BEZUGLOV N.N., KLYUCHAREV A.N., SHEVEREV V.A., *Associative ionization rate constants measured in cell and beam experiments*, Journal of Physics B **20**(11), 1987, pp. 2497–2513.
- [25] DOBROLEZH B.V., KLYUCHAREV A.N., SEPMAN V.YU., *Determination of the rate constant of associative ionization process in optically excited cesium vapor*, Optics and Spectroscopy **38**, 1975, pp. 630–632.
- [26] KLYUCHAREV A.N., BEZUGLOV N.N., MATAVEEV A.A., MIHAJLOV A.A., IGNJATOVIC L.J.M., DIMITRIJEVIC M.S., *Rate coefficients for the chemi-ionization processes in sodium- and other alkali-metal geocosmical plasmas*, New Astronomy Reviews **51**(7), 2007, pp. 547–562.
- [27] PATTERSON B.M., TAKEKOSHI T., KNIZE R.J., *Measurment of photoionization cross section of the $6P_{3/2}$ state of cesium*, Physical Review A **59**(3), 1999, pp. 2508–2510.
- [28] GILBERT S.L., NOECKER M.C., WIEMAN C.E., *Absolute measurement of the photoionization cross section of the excited 7S state of cesium*, Physical Review A **29**(6), 1984, pp. 3150–3153.
- [29] HEINZMANN U., SCHINKOWSKI D., ZEMAN H.D., *Comment on measuring photoionization cross sections of excited states*, Applied Physics A **12**(1), 1977, p. 113.
- [30] PAPPAS D., PIXLEY N.C., SMITH B.W., WINEFORDNER J.D., *Fluorescence monitoring of laser induced population changes of 6P and 6D levels in cesium vapor*, Spectrochimica Acta Part B **55**(9), 2000, pp. 1503–1509.
- [31] CHERET M., BARBIER L., LINDINGER W., DELOCHE R., *Penning and associative ionisation of highly excited rubidium atoms*, Journal of Physics B **15**(19), 1982, pp. 3463–3477.
- [32] MAHMOUD M.A., *Kinetics of Rb_2^+ and Rb^+ formation in laser-excited rubidium vapor*, Central European Journal of Physics **6**(3), 2008, pp. 530–538.

Received April 15, 2009
in revised form June 29, 2009